Journal of the Physical Society of Japan
Vol. 74, No. 6, June, 2005, pp. 1702–1705

Spin-Singlet Ground State in Two-Dimensional $S = 1/2$ Frustrated Square Lattice: $(CuCl)LaNb_2O_7$

H. KAGEYAMA*, T. KITANO, N. OBA, M. NISHI[1], S. NAGAI[1], K. HIROTA[1], L. VICIU[2†], J. B. WILEY[2], J. YASUDA, Y. BABA, Y. AJIRO and K. YOSHIMURA

Department of Chemistry, Graduate School of Science, Kyoto University, Kyoto 606-8502
[1]*Neutron Science Laboratory, Institute for Solid State Physics, University of Tokyo, 106-1 Shirakata, Tokai, Ibaraki 319-1106*
[2]*Department of Chemistry and the Advanced Materials Research Institute, University of New Orleans, New Orleans, LA 70148-2820, U.S.A.*

(Received February 25, 2005; accepted April 6, 2005)

We report on the magnetic properties of double-layered perovskite $(CuCl)LaNb_2O_7$ with a square lattice of $S = 1/2$ Cu^{2+} ions, prepared by topotactic ion-exchange reactions. Magnetic susceptibility exhibits a thermal-activated behavior, and the analysis of the data suggests competing ferro- and antiferromagnetic exchanges for first- and second-nearest-neighbor bonds, respectively. Neutron scattering experiments provide explicit evidence for a spin-singlet ground state with an energy gap of 2.3 meV. The well-defined low-lying triplet mode is almost independent of Q despite densely packed magnetic ions in the CuCl plane. In addition, on the basis of the isolated dimer model, we found that the intradimer distance is as long as 8.8 Å, which corresponds to the fourth-nearest-neighbor bond. These results indicate a sizable geometrical frustration that should impose severe constraints on the propagation of the triplet excitation, as in the case of $SrCu_2(BO_3)_2$. This argument is further reinforced by the observation of a collective-triplets bound state at 5.0 meV.

KEYWORDS: spin gap, square lattice, J_1–J_2 model, ion-exchange reaction, neutron scattering, bound state, $(CuCl)LaNb_2O_7$
DOI: 10.1143/JPSJ.74.1702

In recent years, much attention has been given to low-dimensional antiferromagnetic (AFM) quantum spin systems that have a ground state with no long-range magnetic order and an energy gap in the magnetic excitation spectrum. Among them, the $S = 1/2$ frustrated square lattice AFM system (J_1–J_2 model) is of special importance in light of Anderson's resonating valence bond (RVB) concept to explain high-T_c superconductivity in doped layered cuprates.[1)] An interesting phase diagram with unusual ground states is predicted as a function of the ratio J_2/J_1 between the first- (J_1) and second- (J_2) nearest-neighbor exchange interactions.[2–4)] For $0 < J_2/J_1 < 0.38$, a normal Néel order state is the ground state, while for $J_2/J_1 > 0.55$, a collinear order should develop. For $0.38 < J_2/J_1 < 0.55$, where the effect of the frustration is stronger, a quantum disordered phase with a finite gap is expected. However, so far there has been no experimental verification of the spin-liquid phase in the J_1–J_2 model, apart from CaV_4O_9[5)] and $SrCu_2(BO_3)_2$[6)] structures, which are derivatives of the square lattice. As far as the authors know, three compounds have been suggested as prototypes of the J_1–J_2 model with significant coupling between J_1 and J_2: Li_2VOSiO_4 ($J_1 = 0.56$, $J_2 = 6.3$ K), Li_2VOGeO_4 ($J_1 = 0.82$, $J_2 = 4.1$ K)[7–9)] and $Pb_2VO(PO_4)_2$ ($J_1 = -6$, $J_2 = 9.8$ K).[10)] All of these are, however, magnetically ordered at low temperatures.

Low-temperature topotactic strategies such as intercalation/deintercalation offer effective routes for the design and construction of new two-dimensional (2D) magnetic materials.[11–13)] In this letter, we will demonstrate that a double-layered Dion-Jacobson phase $(CuCl)LaNb_2O_7$, prepared from topochemical ion exchange, provides a new class of 2D Heisenberg spin systems, where a spin-singlet ground state with a finite energy gap is achieved in the $S = 1/2$ frustrated square lattice. The structure of $(CuCl)LaNb_2O_7$, determined using Rietveld analysis of X-ray powder diffraction data,[11)] revealed that the lattice is tetragonal (space group $P4/mmm$), the room-temperature cell constants being $a = 3.879$ Å and $c = 11.728$ Å. As shown in Fig. 1, the structure consists of magnetic CuCl planes widely separated by nonmagnetic double perovskite slabs. Hence 2D magnetic properties are strongly expected. The $S = 1/2$ copper ion is octahedrally coordinated, bridging apical oxygen ions

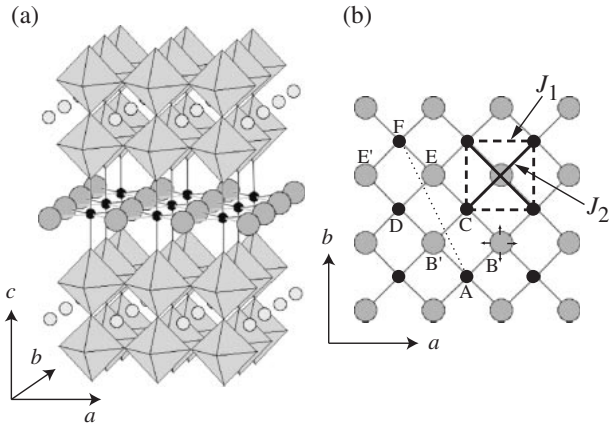

Fig. 1. (a) Structure of $(CuCl)LaNb_2O_7$. The closed spheres are Cu^{2+}, the gray spheres are Cl^-, the open spheres are La^{3+}, and the octahedra represent NbO_6.[11)] (b) The CuCl layer viewed along [001]. The Cu^{2+} ions connected by the dotted line correspond to a 4NN dimer. The bold broken and solid lines represent, respectively, the J_1 and J_2 bonds. Later structural investigation[14)] has suggested disorder of Cl^- ions from 1*a* (0, 0, 1/2) to 4*m* (*x*, 0, 1/2), as indicated by the arrows.

*E-mail: kage@kuchem.kyoto-u.ac.jp
†Present address: Department of Chemistry and Princeton Materials Institute, Princeton University, NJ 08544, U.S.A.

of the perovskite layer and surrounded by four chlorine ions in the CuCl plane. The CuO_2Cl_4 octahedra share corners with the NbO_6 octahedra of the perovskite slabs and edges with other CuO_2Cl_4 octahedra in the CuCl plane. Later structural analysis on the basis of neutron diffraction suggests disorder of the chlorine ions within the CuCl plane.[14)]

The ion-exchange reaction for the synthesis of (CuCl)-$LaNb_2O_7$ is expressed as $RbLaNb_2O_7 + CuCl_2 \rightarrow$ (CuCl)-$LaNb_2O_7 + RbCl$. The details of the synthesis are given in ref. 11. The powder X-ray diffraction pattern indicated a single-phase product with cell parameters consistent with those previously reported.[11)] The energy dispersive spectroscopy (EDS) confirmed a stoichiometric composition. Magnetic susceptibility measurements were performed on a powder sample with a SQUID magnetometer (Quantum Design, MPMS) over the temperature range $T = 2$–$300\,\mathrm{K}$ in an applied field of $H = 0.1\,\mathrm{T}$. Inelastic neutron scattering experiments were carried out on the ISSP-PONTA triple-axis spectrometer installed at a 5G beam port of JRR-3M at the Japan Atomic Energy Research Institute. A powder sample of 12.6 g was put into an aluminum cylinder. Most of the data were collected using a fixed final energy E_f of $14.7\,\mathrm{meV}$ ($k_f = 2.67\,\mathrm{\AA^{-1}}$) and a horizontal collimation of open-40′-S-80′-80′ in combination with a pyrolytic graphite (PG) filter placed after the sample to eliminate higher-order beam contaminations. This setup yields an energy resolution of $1.21\,\mathrm{meV}$ at $Q = 1.38\,\mathrm{\AA^{-1}}$ and $E = 0$, as determined by measuring the incoherent scattering from the sample.

Figure 2 shows the magnetic susceptibility χ for (CuCl)$LaNb_2O_7$. At high T above 50 K, the raw data χ_r exhibit a Curie–Weiss (CW) behavior. On cooling, χ_r exhibits a broad maximum at around 16.5 K (T^{χ}_{max}), which is characteristic of low-dimensional AFM system, and decreases rapidly with decreasing T. This decrease suggests a spin-singlet ground state separated from the excited state by a finite energy gap. It should be noted that neutron diffraction experiments revealed no sign of 3D order. Apart from the pronounced thermal-activated character, a Curie tail is seen below 4 K, most likely due to residual impurities and/or defects of Cu^{2+} ions in (CuCl)$LaNb_2O_7$. The amount of impurities/defects was estimated to be about 2.6% of free $S = 1/2$ Cu^{2+} ions. After subtracting this upturn, one obtains the spin susceptibility χ_s. Subsequently, the analysis of χ_s using the CW formula, $\chi = C/(T + \theta)$, resulted in $\theta_s = 9.6\,\mathrm{K}$ and $C_s = 0.385$ [emu K/mol]. Assuming the stoichiometric composition, as supported by EDS, a reasonable value of 2.03 from the g-factor for a Cu^{2+} ion, g_s, is obtained.[15)]

As a starting point, in order to estimate mainly the spin gap Δ, we first analyzed the χ_s data using a $S = 1/2$ isolated AFM dimer model, where the susceptibility χ_d is precisely expressed as

$$\chi_d = \frac{Ng^2\mu_B^2}{3k_BT}\left[1 + \frac{1}{3}\exp(\Delta/T)\right]^{-1}, \qquad (1)$$

where N, μ_B, and k_B denote Avogadro's number, the Bohr magneton, and Boltzmann's constant, respectively. Here, Δ equals the strength of intradimer interaction J and is the only adjustable parameter in eq. (1). The value of Δ was determined so as to make the temperatures at maximum χ_s and χ_d coincide with each other. As a result, we obtained $\Delta = 26.5\,\mathrm{K}$. Despite the densely arranged magnetic ions in the CuCl layers, χ_d appears to agree well with χ_s. Yet, as seen at around 15 K, a quantitative discrepancy exists between χ_s and χ_d. Furthermore, the $1/\chi$ vs T plots in Fig. 2(b) clearly exhibit a disagreement between experiment and theory at high T.

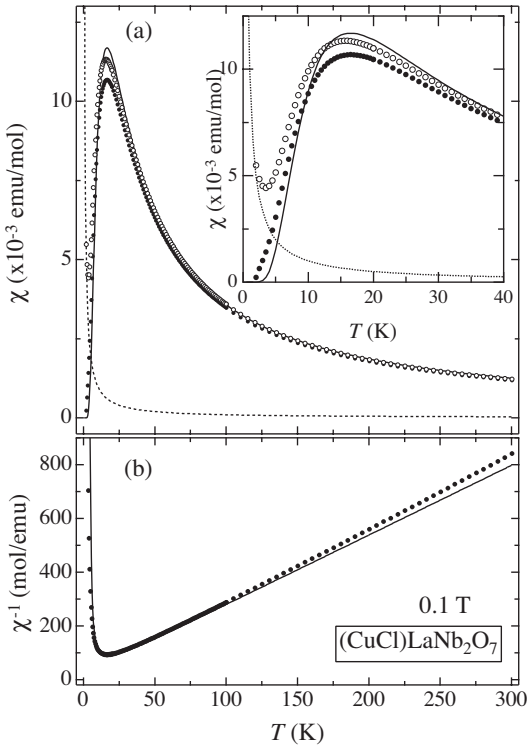

Fig. 2. (a) The T variation of the magnetic susceptibility in (CuCl)-$LaNb_2O_7$ measured at 0.1 T. There is no difference between ZFC/FC susceptibilities. The open and closed circles represent, respectively, χ_r and χ_s, while the dotted line represents the Curie term. The solid line is χ_d with $\Delta = 26.5\,\mathrm{K}$. The enlarged plot is presented in the inset. (b) Reciprocal susceptibilities, $1/\chi_s$ and $1/\chi_d$.

It is known that θ is equal to $J_1 + J_2$ for the J_1–J_2 model. In the limit of $J_1 \gg J_2$ ($J_2 \gg J_1$), χ should be that of the Heisenberg AFM system on the square lattice with only one coupling constant $J_{1(2)}$ and the maximum occurs at $T^{\chi}_{max} \sim 0.935J_{1(2)}$ ($= 0.935\theta$).[16)] The experimental ratio $T^{\chi}_{max}/\theta_s = 1.72$, which is much larger than that for the nonfrustrated case, indicates the presence of significant frustration. It is worth pointing out that the J_2 bonds are always frustrated by the geometry as long as J_2 is AFM. The chlorine ions in the CuCl plane are arranged at the center of 2NN bonds, not 1NN bonds, so that J_2 need not be smaller in magnitude than J_1. The Cu^{2+}–Cl–Cu^{2+} angle of 180° for the J_2 bond actually supports a sizable AFM interaction ($J_2 > 0$), while that of 90° for the J_1 bond points to a ferromagnetic (FM) J_1 (<0). Direct evidence for the FM J_1 is given by the large value of T^{χ}_{max}/θ_s. This is the second example of FM J_1, following $Pb_2VO(PO_4)_2$.[10)] However, $Pb_2VO(PO_4)_2$ exhibits a transition to an ordered state at 3.8 K in contrast with the present compound that shows no 3D order. To date, most of the existing theories based on the J_1–J_2 model concern the cases with AF interactions. There is only one theoretical paper that deals with FM J_1,[17)] in which it was suggested that there should also be a spin-liquid phase occurring for

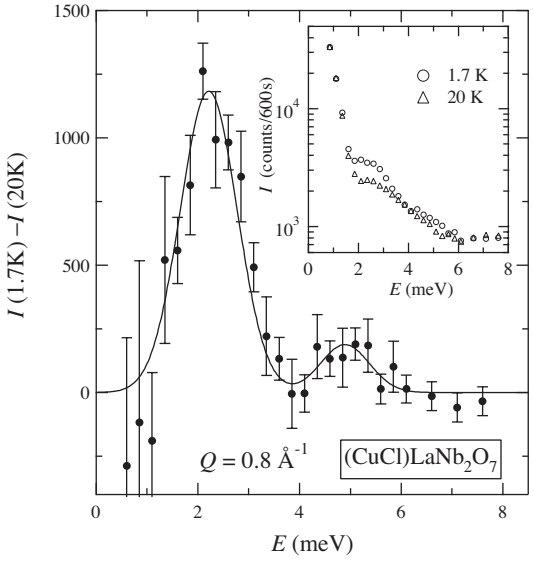

Fig. 3. Inset: constant-Q scan at $0.8\,\text{Å}^{-1}$, $T = 1.7\,\text{K}$ (circles) and 20 K (triangles). The circles in the main panel are the difference, $I(1.7\,\text{K}) - I(20\,\text{K})$. The full curve represents the least-squares fit, where the peaks were approximated by two Gaussians.

$J_2/J_1 \sim -0.5$ between the FM and collinear ordered phases. It is exciting if $(CuCl)LaNb_2O_7$ can be an experimental correspondence of this model.

Let us move onto the result of the neutron scattering experiments. Typical constant-Q scans collected at $T = 1.7$ and 20 K are shown in the inset of Fig. 3. Due to the use of a powder sample and elastic incoherent scattering which progresses moderately below 6 meV and rapidly below 2 meV, relatively weak magnetic scattering from the sample in this E range can be better recognized when the intensity at 20 K, $I(20\,\text{K})$, is subtracted from that at 1.7 K, $I(1.7\,\text{K})$ (see the main panel of Fig. 3). There are two symmetric inelastic peaks indicating magnetic scattering from the spin-singlet ground state, which we call transitions I and II. No other features were observed for energy transfer up to 18 meV. The least-squares fit to the experimental data, where the peaks are approximated by multi-Gaussians, gave the excitation energies of 2.31 ± 0.05 and 5.0 ± 0.3 meV and full widths at half maximum of 1.3 ± 0.1 and 1.2 ± 0.7 meV for transitions I and II, respectively. The widths are as large as the instrumental resolution. The first gap of $\Delta = 2.3$ meV ($\sim$26.7 K) agrees well with that estimated from the χ–T data. The discrepancy below 1 meV, in other words, negative values of $I(1.7\,\text{K}) - I(20\,\text{K})$, most probably reflects paramagnetic scattering which is negligible at 1.7 K but effective at 20 K. The T dependence of the intensity at 2.2 meV and $Q = 0.4\,\text{Å}^{-1}$ is shown in Fig. 4. The intensity decreases with increasing T and levels off at a constant value above approximately 20 K, a temperature comparable to that of the spin gap. These results are consistent with the interpretation that transition I is a one-triplet excitation from the spin-singlet ground state. The origin of transition II will be discussed later.

In order to gain an insight into the dynamical properties of the one-triplet mode, a number of constant-Q scans were performed for $0.4 < Q < 3.2\,\text{Å}^{-1}$. In general, for 2D systems having a spin-singlet ground state, the magnetic

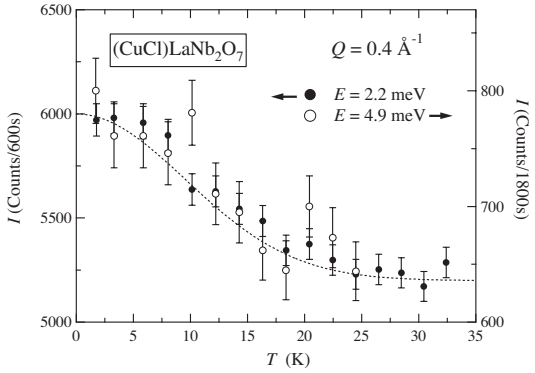

Fig. 4. The T variation of the intensities at $E = 2.2$ meV (left) and 4.9 meV (right), at $Q = 0.4\,\text{Å}^{-1}$. The broken line is a guide for the eyes.

excitations have a wide band and thus a strong dispersion along the magnetic plane. The spectrum shapes at constant E and constant Q depend, to a large extent, on the shape of the dispersion relation. In particular, constant-Q scans through the gap show an extended tail in the high-E region, giving rise to an asymmetric peak shape. However, our results for $(CuCl)LaNb_2O_7$ obviously exhibit different behavior from conventional 2D systems; the most prominent features of the inelastic scattering are that the spectrum shapes in constant-Q scans for transition I are completely symmetric (Fig. 3) and that it is almost independent of Q (ΔE is 0.2 meV at most) [Fig. 5(a)]. This means that there is, at least empirically, no strong two-dimensionality in the magnetic excitations, although the crystal structure reveals a distinct square-lattice arrangement of Cu^{2+} ions. Such a dispersionless band has been typically observed in isolated or weakly coupled AFM clusters, as in dimers,[18,19] and a four-spin cluster.[20] We believe that in $(CuCl)LaNb_2O_7$, the geometrical frustration should play a crucial role in making the one-triplet excitation extremely localized, thus giving rise to the flat dispersion. A similar flat dispersion associated with the frustrated geometry has been observed in the Shastry–Sutherland compound $SrCu_2(BO_3)_2$.[21] The one-triplet ex-

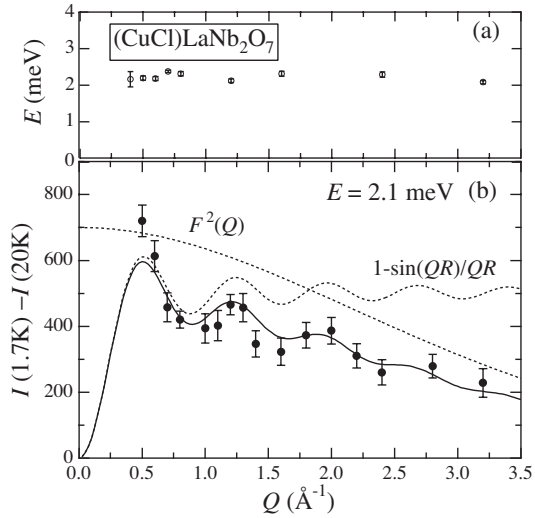

Fig. 5. (a) The Q dependence of transition I. (b) Peak intensities of transition I as a function of Q. The solid line indicates the fit according to eq. (2), which resulted in $R = 8.8\,\text{Å}$.

citations for the Shastry–Sutherland model can propagate only from the sixth order in the perturbation calculations.[22]

In Fig. 5(b), we demonstrate the Q dependence of the scattering intensity, $I(1.7\,\mathrm{K}) - I(20\,\mathrm{K})$, measured at the center of the first energy gap, where an oscillating behavior is clearly seen. In analyzing this data, the use of the isolated dimer model is possible because of the localized character of triplet excitations *irrespective of their origin*.[18,19,21] The intensity of a singlet-to-triplet transition for an isolated dimer is expressed as

$$I(Q) \propto F^2(Q)\left(1 - \frac{\sin QR}{QR}\right), \tag{2}$$

where the last term is the interference term reflecting the separation R within a dimer.[18,19] From the qualitative point of view, not only does the intensity decrease, as expected for $F^2(Q)$,[23] but the modulation due to the interference term is reproduced well. The surprise came from the quantitative analysis; we obtained an extraordinarily long intradimer distance of $R = 8.8\,\text{Å}$[24] which is far longer than 3.879 Å (1NN) and those in usual dimer systems.[18,19] It is rather close to 8.674 Å (4NN). This means that the spin-liquid phase in the present system is essentially different from the columnar dimerized state for the J_1–J_2 model around $J_2/J_1 \sim 0.5$ where the 1NN bonds are responsible for the spin-singlet formation.[2–4]

As to the configuration of the 4NN spin-singlet pairs, there are three possibilities. First, the 4NN pairs may be arranged in an ordered manner, associated with the breaking of the translational symmetry. Although no superstructure reflections were observed in our neutron diffraction profiles down to 1.5 K, a relevant structural modulation might be very subtle. A second scenario is a description based on the static but random distribution of the 4NN pairs in the layer. The problem here is how one particular 4NN bond is chosen out of eight equivalent sites. This may be resolved by considering the disorder of the chlorine ions[14] because it may differentiate otherwise uniform bonds. Last, but not least, is the RVB state, or a resonant mixture of the 4NN pairs, which is possible without any structural phase transition.

Can the original J_1–J_2 model with FM J_1 account for the dimerization of the 4NN bonds? As noted above, a spin-liquid phase for FM J_1 has been proposed to occur between the FM and collinear order phases.[17] Their justifications largely rely on the analogy with the well-investigated spin-liquid phase for AFM J_1 between the Néel and collinear order phases. Therefore, the nature of the new phase remains mostly unidentified as of yet, including the problem of which nearest-neighbor bond forms the spin singlet. Nevertheless, we would like to bring the attention of readers to one important fact: The exchange routes A–(B,B′)–C–E–F and A–B′–D–(E,E′)–F (see Fig. 1(b)) are compatible with AF correlation between 4NN sites. Alternatively, it might be necessary to consider a generalized J_1–J_2 model that includes 3NN (J_3) and 4NN (J_4) bonds, spin–lattice couplings, and randomness effect induced by the disorder of chlorine ions.

Finally, let us briefly discuss the origin of the excitation at 5.0 meV. As shown in Fig. 4, the T dependence of the intensity of transition II shows the same tendency as does that of transition I, indicating that transition II is associated with the collective bound state excitation of several elementary triplets. Note that distinct multitriplet excitations with a similar T dependence have been observed in $SrCu_2(BO_3)_2$.[21] Because the second energy gap 5.0 meV exceeds twice the first energy gap (4.6 meV), transition II should correspond to excitations of more-than-two triplets. If the bound state consists of three elementary triplets, it has considerable stabilization energy, i.e., 1.9 meV, implying strong triplet-triplet interactions present in this system. The reason for the absence of the two-triplet bound state mode remains to be solved.

To summarize, we demonstrated that $(CuCl)LaNb_2O_7$ is a new 2D spin gap system realized for the first time in a $S = 1/2$ frustrated square lattice. The χ–T data indicated a spin-liquid state with competing FM J_1 and AFM J_2. The neutron scattering experiment probed two resolution-limited peaks at 2.3 and 5.0 meV, corresponding to one- and multitriplet excitations, respectively. The dispersion of the former is nearly flat ($\Delta E < 0.2$ meV) and the intensity shows an oscillatory behavior as a function of Q. These phenomena are consequences of the strong geometrical frustration present in the square lattice. It was also shown that the dimer size is as long as the 4NN bond, but the configuration of dimerized pairs in the layer has yet to be determined. We strongly hope that our experiments will trigger intensive theoretical investigations on the (generalized) J_1–J_2 model with FM J_1 for greater understanding of the nature of the spin-liquid phase in $(CuCl)LaNb_2O_7$.

Acknowledgment

We are grateful to Professor F. Mila for his useful comments on the J_1–J_2 model. This work has been supported partly by the National Science Foundation (DMR-0309972).

1) P. W. Anderson: Science **235** (1987) 1196.
2) N. Read and S. Sachdev: Phys. Rev. Lett. **62** (1989) 1694.
3) M. P. Gelfand *et al.*: Phys. Rev. B **40** (1989) 10801.
4) F. Becca and F. Mila: Phys. Rev. Lett. **89** (2002) 037204.
5) K. Kodama *et al.*: J. Phys. Soc. Jpn. **66** (1997) 793.
6) H. Kageyama *et al.*: Phys. Rev. Lett. **82** (1999) 3168.
7) R. Melzi *et al.*: Phys. Rev. Lett. **85** (2000) 1318.
8) R. Melzi *et al.*: Phys. Rev. B **64** (2001) 024409.
9) H. Rosner *et al.*: Phys. Rev. B **67** (2003) 014416.
10) E. E. Kaul *et al.*: J. Magn. Magn. Mater. **272–276** (2004) 922.
11) T. A. Kodenkandath *et al.*: J. Am. Chem. Soc. **121** (1999) 10743.
12) T. A. Kodenkandath *et al.*: Inorg. Chem. **40** (2001) 710.
13) H. Kageyama *et al.*: J. Phys.: Condens. Matter **16** (2004) S585.
14) G. Caruntu *et al.*: Mater. Res. Bull. **37** (2002) 593.
15) The fitting of χ_r to the CW law gave similar values of $\theta_r = 9.5$ K and $C_r = 0.398$ emu K/mol corresponding to $g_r = 2.06$.
16) J.-K. Kim and M. Troyer: Phys. Rev. Lett. **80** (1998) 2705.
17) N. Shannon *et al.*: Eur. Phys. J. B **38** (2004) 599.
18) A. Furrer and H. U. Güdel: Phys. Rev. Lett. **39** (1977) 657.
19) H. U. Güdel *et al.*: Inorg. Chem. **18** (1979) 1021.
20) M. Hase *et al.*: Phys. Rev. B **56** (1997) 3231.
21) H. Kageyama *et al.*: Phys. Rev. Lett. **84** (2000) 5876.
22) S. Miyahara and K. Ueda: Phys. Rev. Lett. **82** (1999) 3701.
23) *International Tables for Crystallography*, ed. A. J. C. Wilson, (Kluwer, Dordrecht) Vol. C, Chap. 4.4.5.
24) On the basis of the isolated dimer model, the cross section has a maximum at $Q = 1.503 \times \pi/R$. Given $R = 8.8$ Å, the maximum should be obtained at $Q = 0.54\,\text{Å}^{-1}$. The present experimental conditions, however, involve an increasing statistical error of the intensity, particularly below $Q \sim 0.5\,\text{Å}^{-1}$.